

Flexible Microstrip Patch Antenna Design on Jeans Substrate Radiating at 2.45 GHz for WBAN Application

Saikumar Mulkalla¹, Avish Fakirde¹, Paritosh D. Peshwe^{1*}

¹Department of Electronics and Communication Engineering, Indian Institute of Information Technology, Nagpur, Maharashtra

Corresponding Author: paritoshpeshwe@gmail.com

Abstract— This study presents a compact, low-profile, and flexible fabric antenna specifically designed for on-body Wireless Body Area Networks operating within the Industrial, Scientific, and Medical (ISM) frequency band at a central frequency of 2.45 GHz. The proposed antenna employs a jeans substrate, with a dielectric constant $\epsilon_r = 1.67$ and loss tangent $\tan\delta = 0.025$, which is 0.5 mm in thickness, allowing for its flexibility. The antenna incorporates slots on the patch and a Defected Ground Structure (DGS), with a total size of $36 \times 55 \times 0.6 \text{ mm}^3$ ($0.29\lambda_o \times 0.45\lambda_o \times 0.005\lambda_o \text{ mm}^3$). To assess the antenna's flexibility, bending analysis was performed, while its performance was evaluated using a phantom model that simulates human tissue, comprising skin, fat, and bone, with respective thicknesses of 1 mm, 0.5 mm, and 4 mm. The final model of the antenna operates at a central frequency of 2.45 GHz, with an impressive bandwidth of 0.8 GHz. The proposed design maintains a high level of directivity, gain, and Reflection Coefficient (S_{11}) at the desired frequency, with values of 4.7 dBi, 3.6 dBi, and -41 dB, respectively. The Specific Absorption Rate (SAR) of the final antenna was measured on the above model and found to be 0.114 W/Kg for 1g of tissue, which is well within the limits established by IEEE and FCC standards. Both the measured and simulated values of return loss and gain suggest that the proposed antenna is eminently suitable for body-worn applications.

Keywords: Flexible Antenna · Wireless Body Area Networks (WBAN) · Jeans Substrate · Defected Ground Structure (DGS) · MicroStrip Patch Antenna · ISM Frequency Band · SAR

1 Introduction

A Wireless Body Area Network (WBAN) is a wireless network that employs wearable devices to monitor and transmit various physiological signals. WBANs have garnered considerable attention in recent years owing to their potential applications in healthcare [1], sports [2], and entertainment [3]. The antenna plays a critical role in a WBAN as it is responsible for transmitting and receiving data between the wearable devices and the network. However, traditional antennas are often rigid, causing discomfort when worn for extended periods, thereby limiting their potential use in wearable devices.

Flexible antennas offer a promising solution for comfortable and continuous monitoring of physiological signals in wearable technology. They are lightweight, conform to the body's shape, and are crafted using flexible materials. These materials are finding applications in the advancement of implantable devices used in healthcare, such as endoscopy, neural recording, glucose monitoring, and intracranial pressure monitoring [4]. Their incorporation allows for improved functionality and performance in these critical healthcare areas.

Antennas are classified into wired and planar types based on their physical structure. Wired antennas, such as straight wire, loop, or dipole antennas, are low-cost but unsuitable for flexibility. Planar antennas are preferred for flexibility due to their ability to conform to surfaces, lightweight nature, low profile, and high performance. Among the available planar antennas, the microstrip patch antenna stands out as the best option for flexible antenna design, owing to its low profile, lightweight construction, ease of manufacturability, and versatility across various applications, including wearables, biomedical sensors, and portable devices. The microstrip patch antenna's planar structure, miniaturization, and stable performance on the human body make it particularly popular in wearable antenna design [5].

Literature has provided different types of flexible and wearable antennas that have been studied over the years. In a study conducted by the authors of [6], a quasi-yagi antenna resonating at 1.5835 GHz was designed. While the antenna was found to be a compact and efficient directive radiator, the substrate used was not ideal for a flexible antenna. Another study by the authors of [7] focused on designing a compact and flexible slot antenna with potential for improved

gain and specific absorption rate (SAR). A low-profile triangular patch antenna with a Koch fractal design was designed in [8], offering a compact size but with a limitation of little impedance fractional bandwidth (7.75% at the resonate frequency of 2.45 GHz). A meander-line antenna was also designed in [9] for head imaging, but the overall dimensions were found to be too large for use in compact environments. Finally, a compact planar dipole antenna having center frequency at 2.47 GHz was proposed in [10], but was limited by its large overall dimensions and minimal gain. These antenna designs have certain limitations, such as increased size, thickness, narrower bandwidth, and higher back radiation, which restrict their suitability for flexible and wearable devices.

The utilization of textile materials as substrates for antennas is increasingly becoming popular, particularly in the context of wearable medical devices. Textile antennas provide a flexible and comfortable solution when integrated into a patient's clothing, ensuring that monitoring data remains unaffected while offering enhanced convenience [11]. Jeans material is a suitable choice for patch antenna design due to its high flexibility, availability, high dielectric constant, and low loss tangent, which contribute to the antenna's good performance. Additionally, jeans material is low-cost, easy to manufacture, and more durable compared to other substrates such as cotton and paper.

In [12], a patch antenna with a partial ground plane on a substrate made of jeans material was designed. However, the measurements of the antenna were quite large, and it exhibited lower gain at lower frequencies. Similarly, [13] describes an inverted F antenna on jeans substrate, but with a relatively low gain that could be improved and [14] presents a PIFA antenna designed on a jeans substrate, but its radiation efficiency is low.

This study focuses on the design and evaluation of a flexible antenna integrated with a Defected Ground Structure (DGS), which was implemented on a Jeans substrate. The main objective was to assess the effectiveness and safety of this newly proposed antenna. Notably, this antenna boasts a thinner profile compared to previous models, and it was found to exhibit a Specific Absorption Rate (SAR) that falls well below the limits set by FCC and IEEE Standards, ensuring compliance with safety regulations [15].

The structure of this paper is as follows: In Section II, a comprehensive explanation is provided regarding the design of the antenna, along with the iterative process employed to achieve the final topology of the proposed antenna. Section III focuses on the Simulation and Performance Analysis of the finalized antenna. Finally, in Section IV, the study concludes by summarizing the key findings and drawing meaningful conclusions from the research conducted.

2 Antenna Design

In [16], various substrate materials were discussed for antenna fabrication, and it was determined that a Jeans material (with $\epsilon_r = 1.67$ and loss tangent = 0.025) having a thickness of 0.5 mm was used as a substrate to achieve the desired flexibility for the antenna. A 50Ω transmission line backed with a defected ground structure (DGS) was employed to excite the radiating element. To begin with, the measurements of the patch and feed were determined by applying standard equations specifically developed for microstrip patch antennas, as outlined in [17]. The ultimate configuration of the antenna represents a modified version of the regular patch antenna. Notably, the ground plane was altered, and slots were etched into it to achieve resonance at the intended frequency and attain substantial gain.

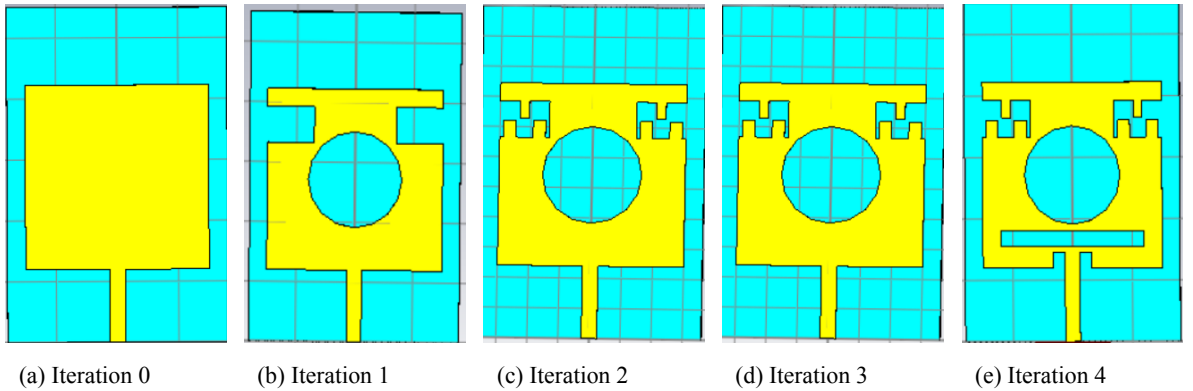


Figure 1: Evolution of patch from iteration 0 to iteration 4

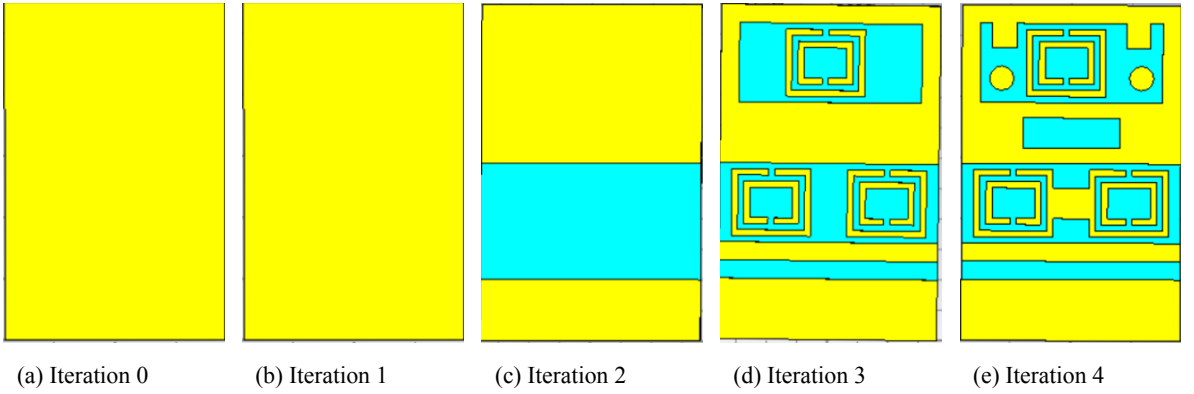


Figure 2: Evolution of ground plane from iteration 0 to iteration 4

The design process began with the conventional patch antenna with a full ground in iteration 0 as shown in Figure 1a and 2a. This antenna had a resonance at around 3.732 GHz and a gain of 0.377 dBi. To shift the resonance to the desired frequency, the antenna was modified in iteration 1 as shown in Figure 1b and 2b, by etching a circular slot and two rectangular slots on the patch to divert the current path, thereby increasing the electrical length of the antenna and shifting the resonance to the left. At this iteration, the antenna resonated at 2.48 GHz, but the S11 value was not below -10 dB, and the gain was also negative. To make the S11 value below -10 dB, impedance matching was required and the DGS structure could significantly improve the gain of the antenna [18]. Therefore, The antenna design underwent modifications from iteration 1 to iteration 2 as shown in Figure 1c and 2c by placing extra copper in the top rectangular slots so that the effective gap decreased, and a rectangular slot was cut down in the ground. These slots increase the capacitance of the antenna, which matched the impedance and the DGS improved the gain. At this iteration, the antenna resonated at 2.04 GHz, the S11 was below -10 dB, and it had a better gain than the previous iteration.

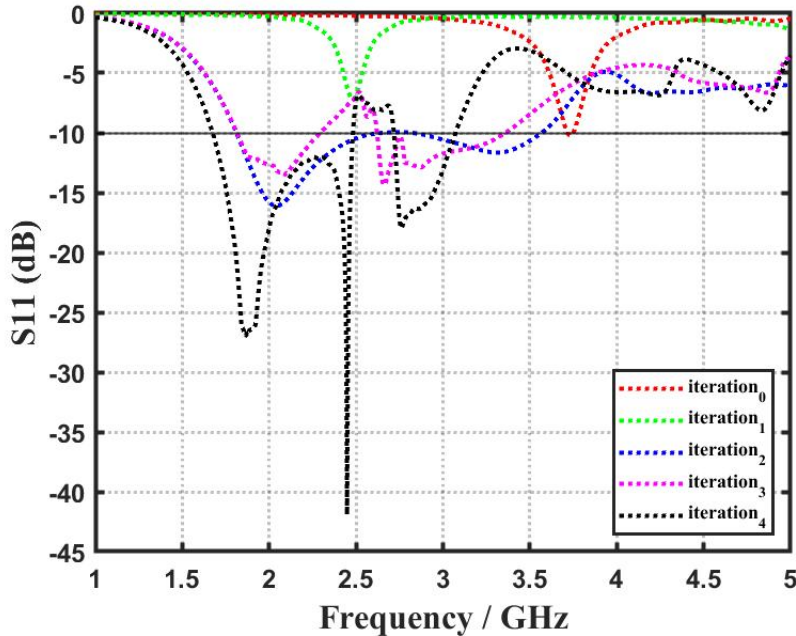


Figure 3: Variation of reflection coefficient (S11) with iterations

To shift the resonance to 2.45 GHz, iteration 3 introduced further modifications to enhance the antenna design previously modified in iteration 2 as shown in Figure 1d and 2d by placing split-ring resonators on the ground plane. Split-ring resonators can act as an artificial magnetic conductor (AMC) when placed on a grounded dielectric substrate. The addition of extra copper reduced the capacitance, shifting the resonance to the right while maintaining or improving the gain. In this iteration, the antenna resonated at 2.66 GHz, the S11 was below -10 dB, and it had a gain of 3.66 dBi. The antenna was further modified in iteration 4 as shown in Figure 1e and 2e by etching a horizontal rectangular slot and two small slots beside the feed the patch. The ground plane was modified by adding copper between and adjacent to the split rings. These slots contributed to an increase in capacitance and electrical length of the antenna, resulting in the antenna resonating at the desired frequency.

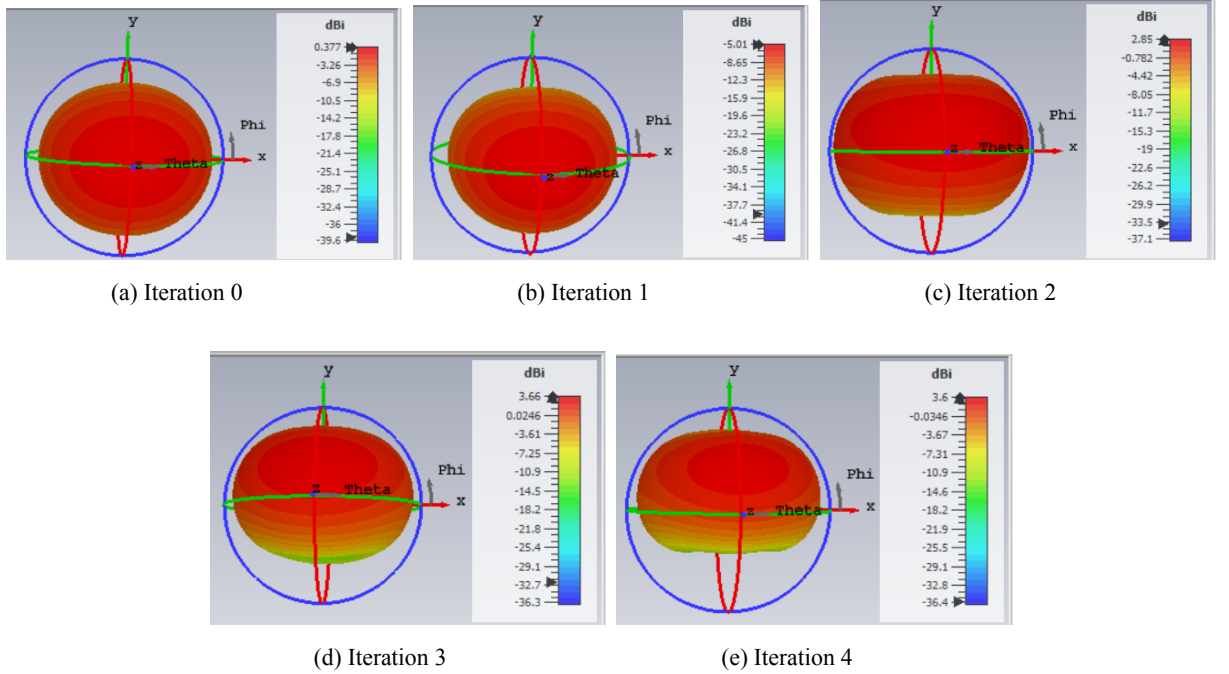


Figure 4: Variation of radiation pattern (gain) of antenna from iteration 0 to iteration 4

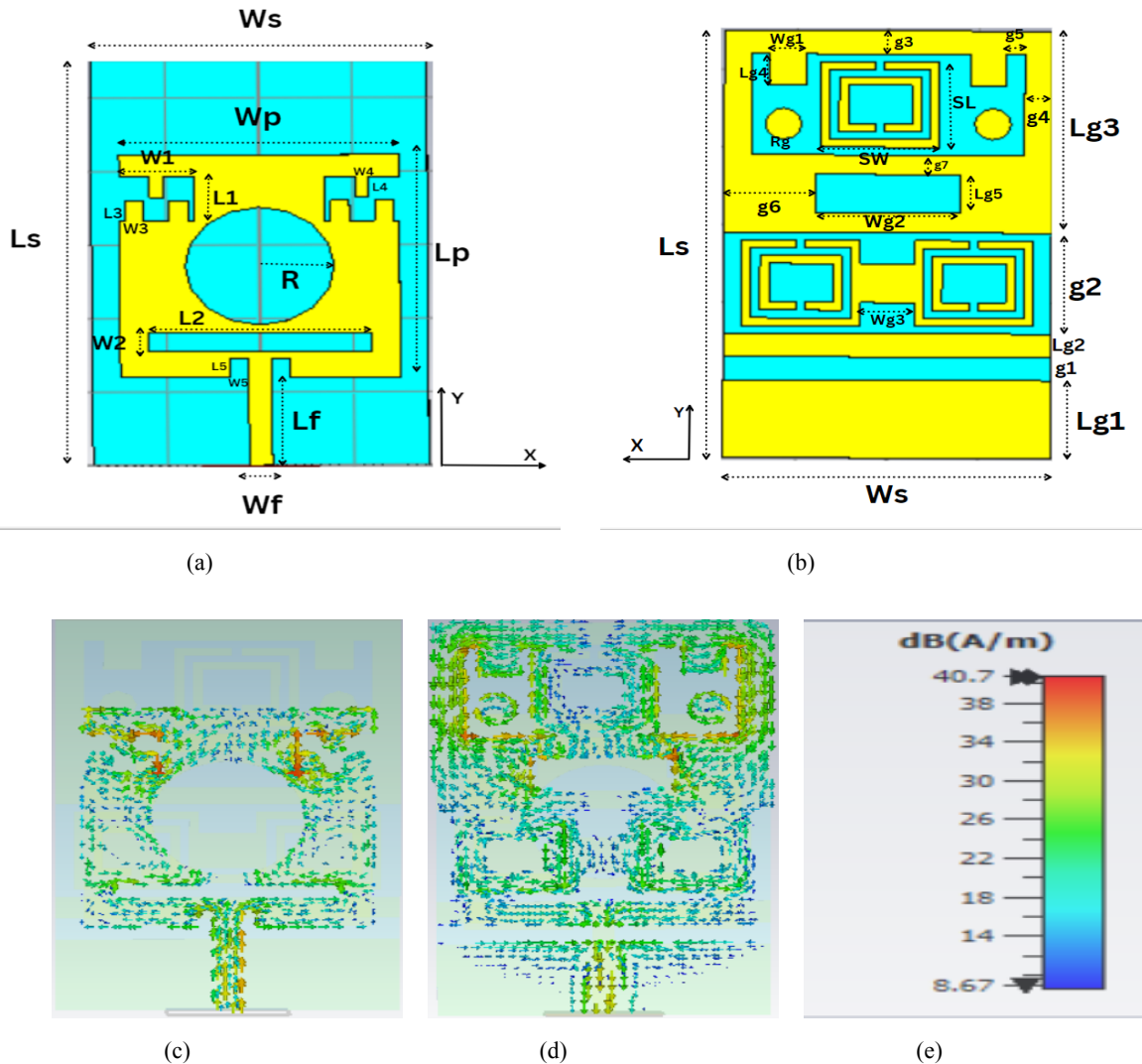


Figure 5: (a) Top view, (b) Bottom view, and surface current distribution (c), (d), and (e) of the final proposed antenna at 2.45 GHz.

In the fourth iteration, which corresponds to the proposed antenna design, resonance was achieved at a frequency of 2.45 GHz. This design exhibited a -10 dB bandwidth ranging from 1.68 GHz to 2.48 GHz, with an S11 value of -41 dB specifically at the resonant frequency of 2.45 GHz. Moreover, the antenna showcased a fractional bandwidth of 38.5% and a peak gain of 3.6 dBi. The proposed antenna exhibits overall dimensions of 36 mm x 55 mm x 0.6 mm ($0.29\lambda_o$ mm x $0.45\lambda_o$ mm x $0.005\lambda_o$ mm). The design evolution steps of the patch and ground plane, along with their corresponding S11 and gain of the antenna, are illustrated in Figures 1, 2, 3 and 4 respectively. Figures 5a and 5b exhibit the superior top and bottom views of the proposed antenna, respectively. Table 1 presents the optimized attributes of the antenna obtained after the final iteration. Figures 5c, 5d, and 5e aptly showcase the surface current density of the antenna at the 2.45 GHz frequency.

Table 1
Optimized design parameters of proposed antenna in Figure 5a and 5b

Dimensions (unit: mm)							
W _s = 36	L _s = 55	W _p = 30	L _p = 30.25	W _f = 2.5	L _f = 12	W ₁ = 8	L ₁ = 6
W ₂ = 2.5	L ₂ = 24	W ₃ = 2	L ₃ = 2.8	W ₄ = 1.5	L ₄ = 2.8	W ₅ = 2	L ₅ = 2.5
R = 8	L _{g1} = 10	L _{g2} = 3	L _{g3} = 26	L _{g4} = 4	L _{g5} = 5	W _{g1} = 4	W _{g2} = 16
W _{g3} = 6	g ₁ = 3	g ₂ = 13	g ₃ = 3	g ₄ = 3	g ₅ = 2	g ₆ = 10	g ₇ = 2.5
SL = 11	SW = 13	R _g = 2	h = 0.5			t = 0.05	

3 Performance Analysis of Proposed Antenna

The antenna was simulated using the Computer Simulation Technology (CST) software. Figures 6a and 6b depict the fabricated antenna. The investigation of its on-body performance was conducted by establishing a three-layer human tissue phantom model measuring 30 mm x 45 mm x 5.5 mm in CST Microwave Studio, as illustrated in Figure 7. The details of the phantom model are listed in Table 2. The proposed antenna was tested on a Vector Network Analyzer, as shown in Figure 8.

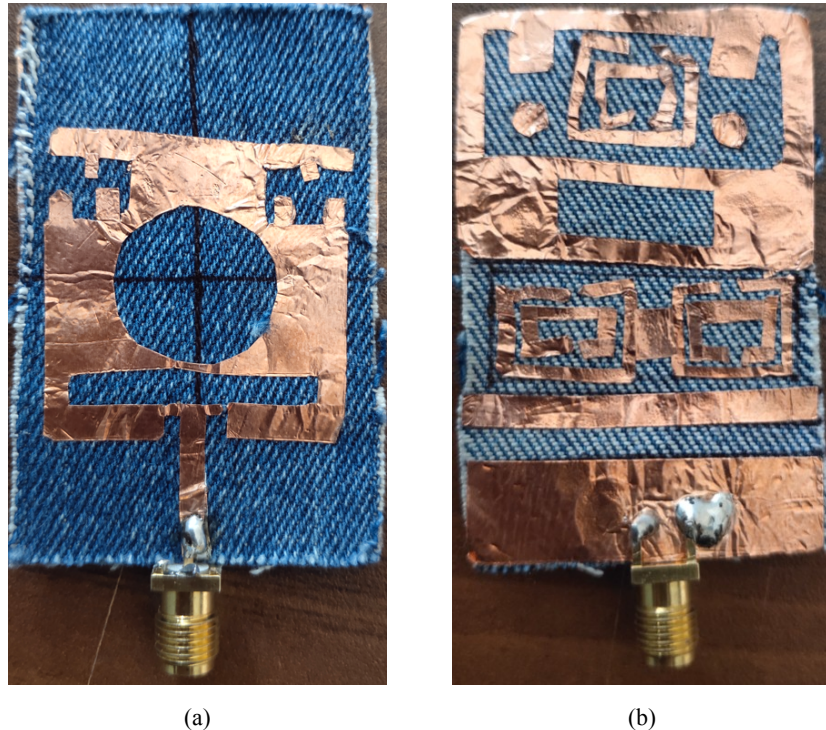


Figure 6: Fabricated proposed antenna (a) top view and (b) bottom view

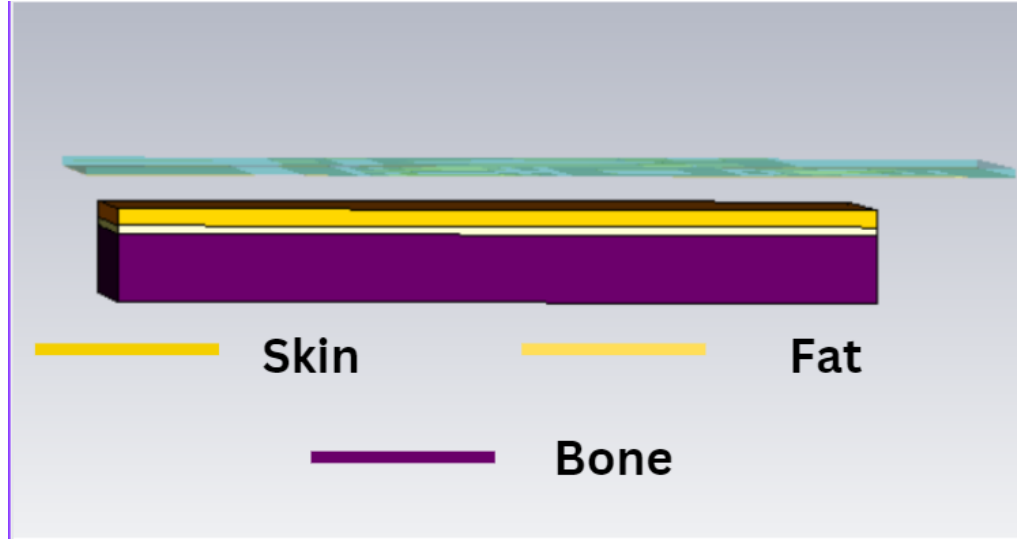


Figure 7: Human tissue phantom model

Table 2
Properties of human tissue phantom model

Tissue	Skin	Fat	Bone
Dielectric Constant (ϵ)	36.6	10.4	16.9
Conductivity [σ (S/m)]	2.34	0.502	1.4
Density [ρ (kg/m³)]	1060	900	1300
Thickness (mm)	1	0.5	4

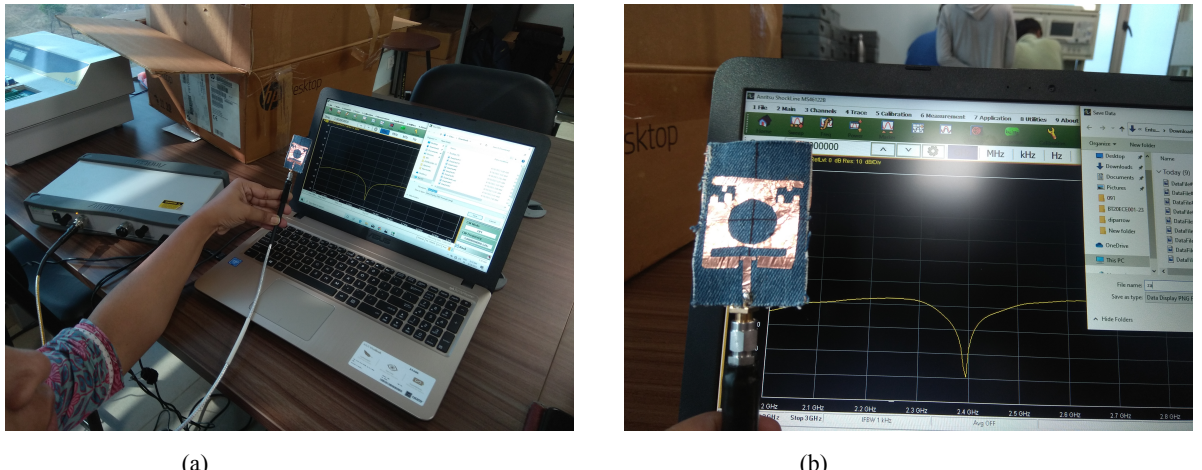


Figure 8: Testing of proposed antenna on VNA

3.1 S11 Parameter

Figure 9 illustrates the simulated, measured and human tissue phantom model S11 values of the proposed antenna. The simulated S11 at 2.45 GHz is -41 dB with a -10 dB impedance bandwidth of 0.8 GHz (1.68 GHz to 2.48 GHz) and a fractional bandwidth of 38.5%. The measured S11, while slightly differing from the simulated values, still demonstrates a band of 2.4 – 2.5 GHz, with a value of -22 dB at 2.45 GHz. The difference between these values can be attributed to fabrication and soldering errors. However, both results suggest that the proposed antenna meets the requirements of the ISM frequency band. Furthermore, the antenna was tested on a human tissue phantom model, yielding an S11 value of -17.5 dB at 2.5GHz with a -10 dB impedance bandwidth of 1.208 GHz (1.552GHz to 2.76 GHz) and a fractional bandwidth of 56%, fulfilling the necessary requirements. Notably, the S11 responses of the examined antenna on the human

tissue phantom model demonstrate a remarkable correspondence with the measured S11 values, indicating a consistent and reliable performance.

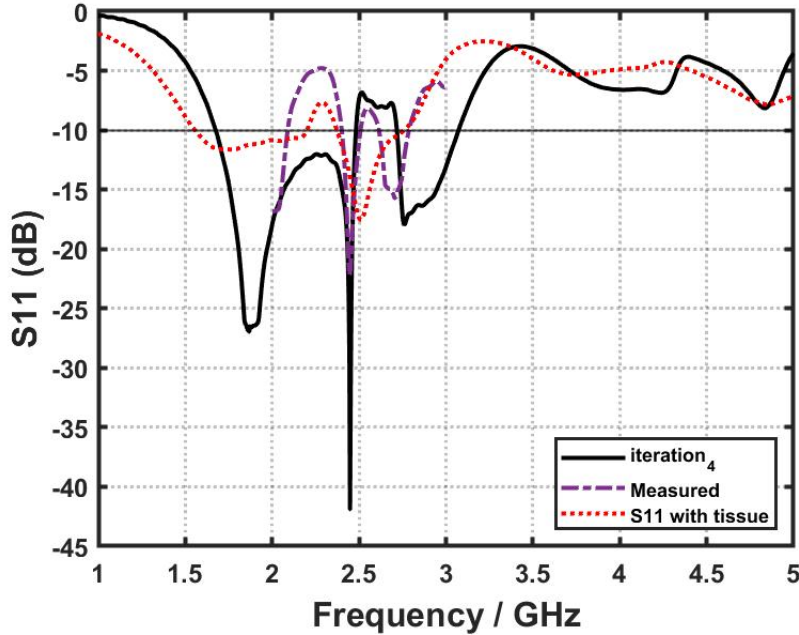


Figure 9: Simulated, measured and with human tissue reflection coefficient (S11) of proposed antenna

3.2 Gain and Radiation Efficiency

The proposed antenna exhibited a maximum gain of 3.6 dBi at 2.45 GHz, coupled with a radiation efficiency of 77.7%, as illustrated in Figure 10. The gain values derived from both practical measurements and computational simulations of the antenna showcased remarkable consistency. The radiation patterns of the antenna in the E-plane ($\phi = 0^\circ$) and H-plane ($\phi = 90^\circ$) were portrayed in Figures 11a and 11b, respectively, both in simulation and measurement.

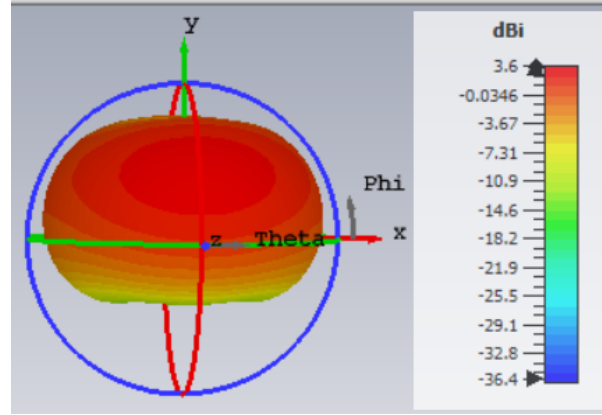


Figure 10: Gain of the proposed antenna

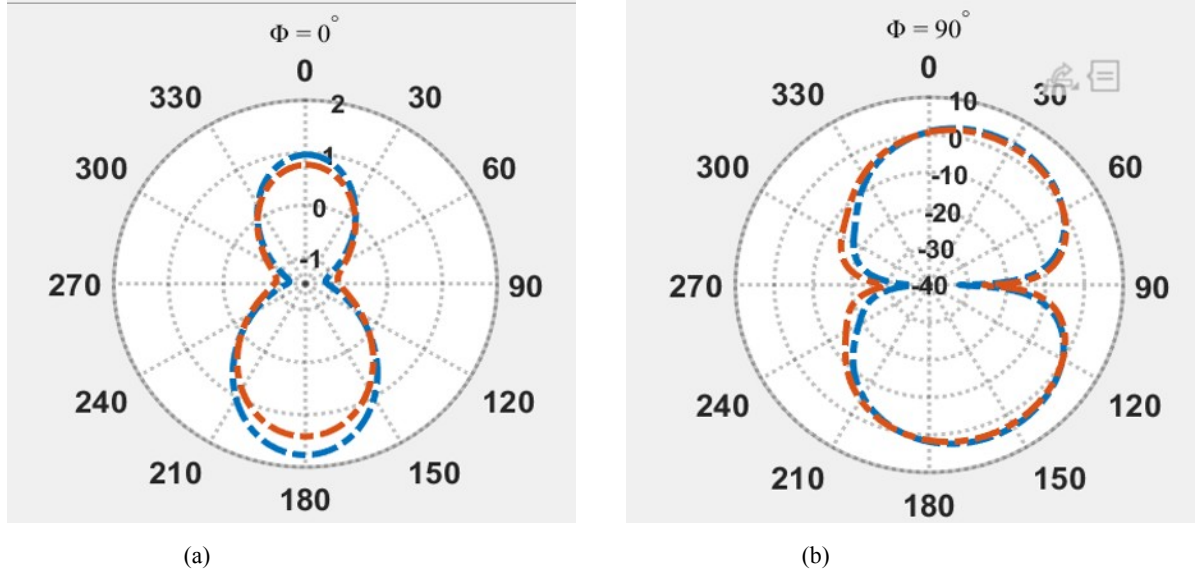


Figure 11: Radiation patterns of the designed antenna in the E-plane ($\phi = 0^\circ$), and (b) in the H-plane ($\phi = 90^\circ$).

3.3 Specific Absorbtion Rate (SAR)

It is necessary to determine the SAR prior to using any antenna in a Wireless Body Area Network (WBAN) to ensure that it complies with safety limits [19].

The Specific Absorption Rate (SAR) measures the absorption of electromagnetic energy by the human body when exposed to RF-EMF. It is expressed in W/kg and calculated as $SAR = (\sigma E^2) / \rho$, where σ is tissue conductivity (S/m), E is electric field strength (V/m), and ρ is tissue density (kg/m^3).

To mitigate the potential hazards associated with harmful radiation, the International Commission on Non-Ionizing Radiation Protection (ICNIRP) has established regulatory limitations. These guidelines stipulate that the Specific Absorption Rate (SAR) should not surpass 2.0 W/kg for 10 grams of tissue. Likewise, the Federal Communications Commission (FCC) has mandated a SAR limit of 1.6 W/kg for 1 gram of tissue.

To evaluate the suitability of the proposed antenna for on-body applications, the SAR was measured on a three-layered human tissue model with a 2 mm offset between the antenna and the model, as illustrated in Figure 12. The SAR value was found to be 0.114 W/kg for 1g of tissue, which falls well within the limits set by the FCC and IEEE standards. Based on these results, it can be concluded that the proposed antenna is well-suited for on-body use.

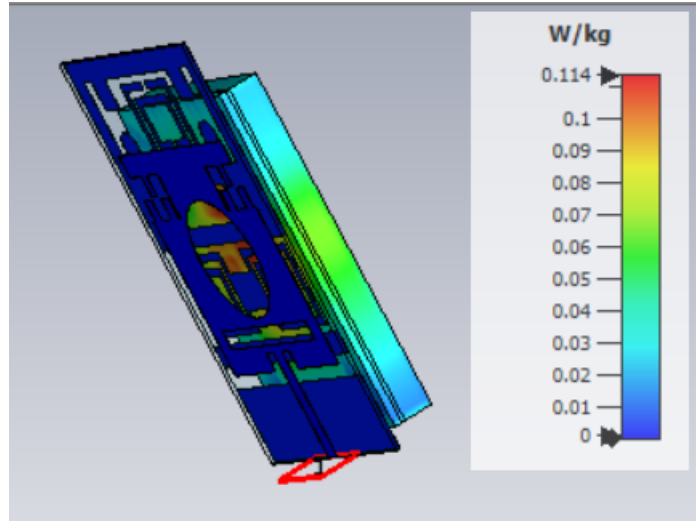


Figure 12: Measured SAR value of the proposed antenna

3.4 Bending Analysis

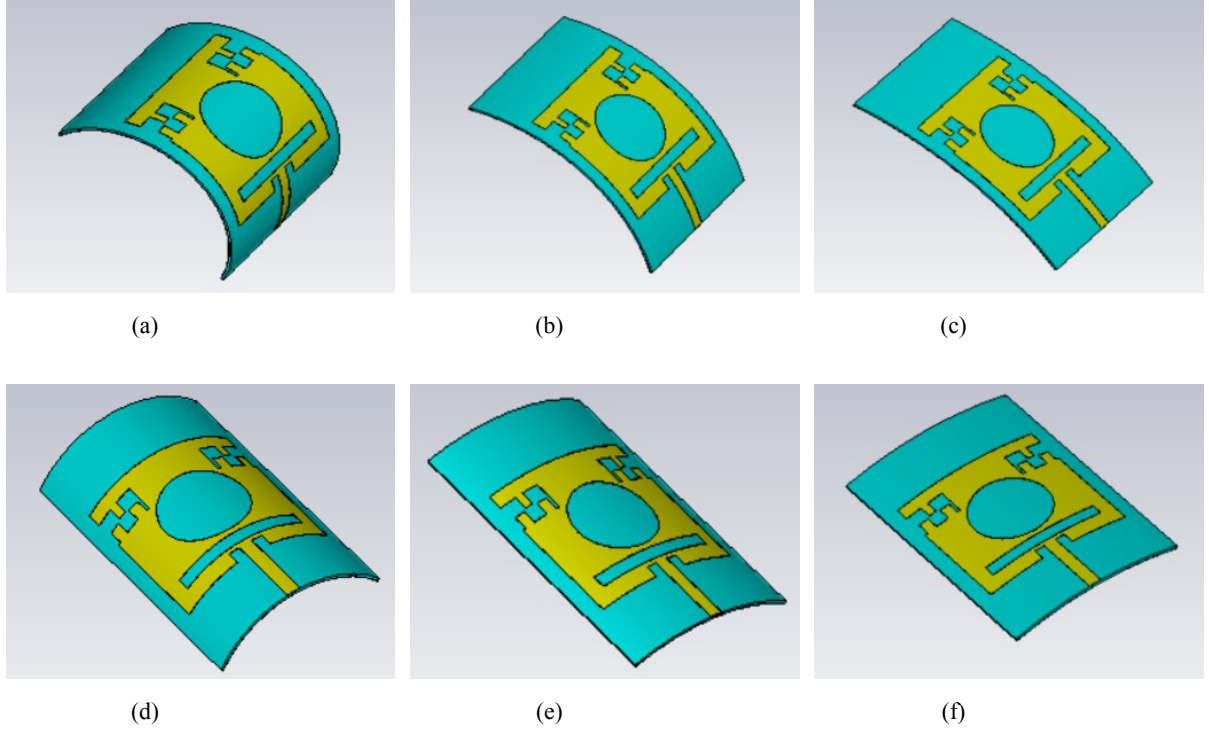


Figure 13: Structure of antenna under two bending condition with different radii, horizontal (x-axis) (a) $R_x = 20$ mm, (b) $R_x = 40$ mm, (c) $R_x = 80$ mm and Vertical (y-axis) (d) $R_y = 20$ mm, (e) $R_y = 40$ mm, (f) $R_y = 80$ mm

In scenarios where antennas are worn on the body, it is anticipated that they will undergo bending during use. This section presents an analysis of the antenna's performance under two bending conditions: vertical (y-axis) and horizontal (x-axis), with varying curvatures. The antenna's S11, gain, and radiation pattern were studied by analysing different radii ($R_x = 80$ mm, 40 mm, 20 mm, $R_y = 80$ mm, 40 mm, 20 mm) along the x-axis and y-axis. The proposed antenna's structure, S11, and radiation patterns under different bending conditions in the x-axis and y-axis are illustrated in figures 13, 14, 15 and 16, respectively.

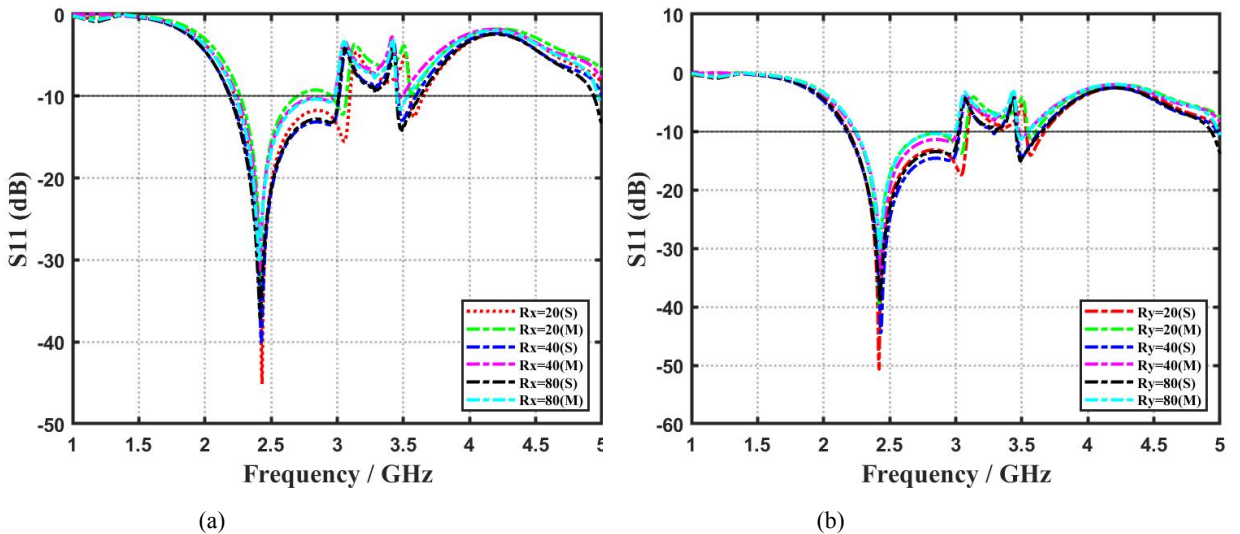


Figure 14: Measured and simulated $S_{11}(s)$ of the proposed antenna under (a) horizontal (x-axis) and (b) vertical (y-axis) bending conditions with different curvatures

The resonance frequency for all bending scenarios exhibited minimal change, indicating that the antenna's performance is not significantly affected by bending. Moreover, the radiation patterns of the antenna remained undistorted under bending scenarios at 2.45 GHz. The antenna's gain improved under the bending scenarios. Under all bending conditions, the antenna was well-matched at the targeted ISM (2.45) band. Based on this study, the proposed antenna has the

potential to be utilized in applications where bending may occur.

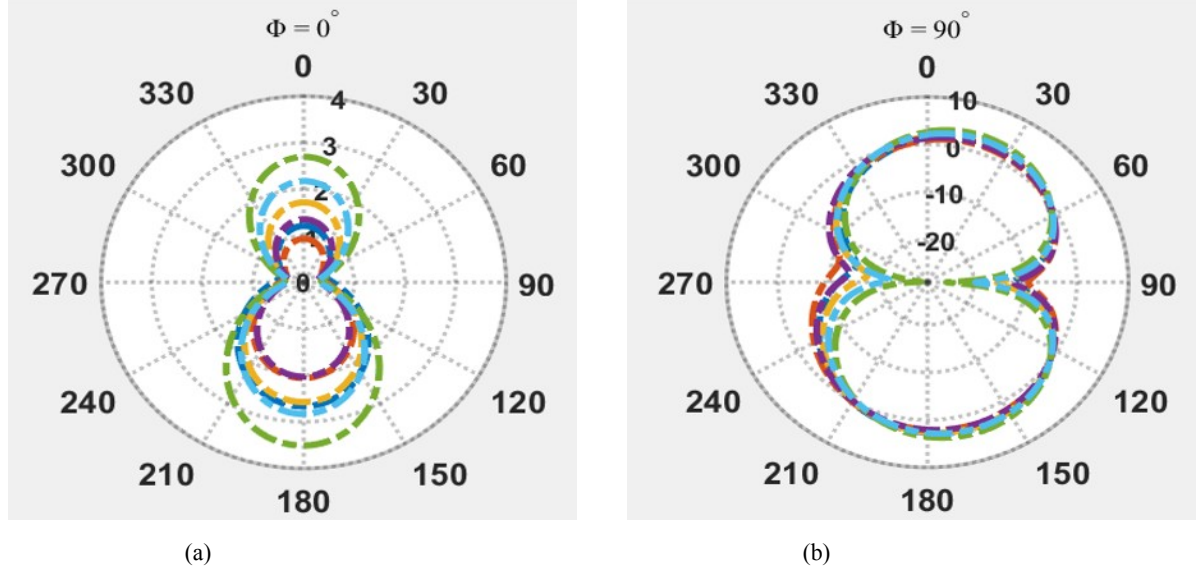


Figure 15: Radiation patterns of the designed antenna under horizontal (x-axis) bending condition in the (a) E-plane ($\phi = 0^\circ$) and (b) H-plane ($\phi = 90^\circ$)

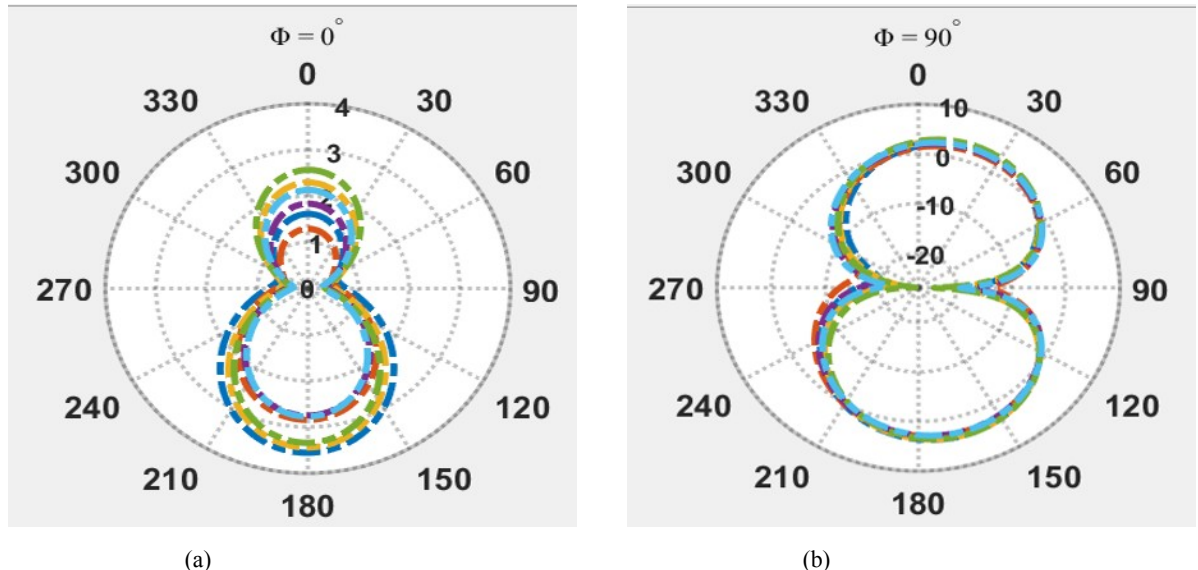


Figure 16: Radiation patterns of the designed antenna under vertical (y-axis) bending condition in the (a) E-plane ($\phi = 0^\circ$) and (b) H-plane ($\phi = 90^\circ$)

Table 3 provides a comprehensive comparison of the antenna's performance in both unbent and bent conditions. Additionally, the study concludes that the proposed antenna is flexible.

Table 3
Comparison of antenna properties under two bending conditions with different curvatures

Bending in x-axis (Horizontal)				Bending in y-axis (Vertical)			
R_x (mm)	Res. freq (GHz)	S11 (dB)	Gain (dBi)	R_y (mm)	Res. freq (GHz)	S11 (dB)	Gain (dBi)
Unbent	2.45	-41	3.6	Unbent	2.45	-41	3.6
20	2.43	-45.14	3.84	20	2.42	-50	3.94
40	2.424	-40	3.78	40	2.43	-44.5	3.89
80	2.415	-37.13	3.82	80	2.424	-39	3.9

3.5 Comparision of the proposed antenna with previous work

To assess the effectiveness of the proposed antennas, a comparative analysis was carried out with existing wearable antennas, as detailed in Table 5.3. The evaluation parameters included size, substrate material and Bandwidth. Based on the analysis, the proposed antenna was found to be relatively compact, exhibited satisfactory radiation performance, and complied with the prescribed SAR limits.

Table 4
Comparision of proposed antenna with other wearable antennas

Ref.	Dimensions (mm ³)	Frequency (GHZ)	S11 (dB)	Gain (dBi)	Substrate
[20]	70 x 70 x 2.26	2.36-2.40	-30	1.38	wolf felt
[21]	70 x 50 x 0.66	1.198-4.055	-26	2.9	Polyester fibre
[22]	59.8 x 59.8 x 3.18	2.3-2.68	-20	2.64	pdms
[23]	85.5 x 85.5 x 5.62	1.4-2.4	-16	1.94	kelver
[24]	38.1 x 38.1 x 2	2.4-2.485	-35	2.79	felt
[25]	40 x 40 x 1.6	1.71-3.94	-30.1	1.96-2.36	fr4
[26]	72.54 x 72.54 x 1.67	2.4-2.5	-18, -23	1.92, 2.27	Felt & jeans, Felt & teflon
Proposed Antenna	36 x 55 x 0.6	1.68-2.48	-41	3.6	jeans

4 CONCLUSION

We have developed a compact, low-profile, and highly flexible fabric antenna suitable for use in Wireless Body Area Networks. The miniaturization and impedance matching of the antenna have been achieved through the incorporation of rectangular and circular slots in the conventional rectangular patch. The gain of the antenna has been further improved through the use of a DGS ground plane. The antenna is resonant at 2.45 GHz with a reflection coefficient of -41dB. Additionally, the designed antenna has a gain of 3.6dBi, with a radiation efficiency of 77.7%. It also demonstrates exceptional performance when subjected to bending along both the x and y axes. Furthermore, the antenna complies with the strict SAR guidelines outlined by both the IEEE and FCC regulatory bodies. Overall, the proposed design exhibits superior performance and represents a highly promising solution for use in human wearable devices.

Statements and Declaration (Acknowledgment)

Funding: No funders are available.

Conflict of Interest/Competing interests: The authors declare no competing interests.

Availability of data and material: All the data generated during and/or analyzed during the current study are available from the corresponding author on reasonable request.

References

- [1] Crosby GV, Ghosh T, Murimi R, Chin CA. Wireless body area networks for healthcare: A survey. International Journal of Ad Hoc, Sensor & Ubiquitous Computing. 2012 Jun 1;3(3):1.
- [2] Fu, Yu & Liu, Jian. (2013). Monitoring System for Sports Activities Using Body Area Networks. Proceedings of the 8th International Conference on Body Area Networks, BodyNets 2013. 408-413. 10.4108/icst.bodynets.2013.253675.
- [3] Sun, Y., Greaves, D.A., Orgs, G., de C. Hamilton, A.F., Day, S. and Ward, J.A., 2023. Using Wearable Sensors to Measure Interpersonal Synchrony in Actors and Audience Members During a Live Theatre Performance. Proceedings of the ACM on Interactive, Mobile, Wearable and Ubiquitous

- Technologies, 7(1), pp.1-29.
- [4] A. Smida, A. Iqbal, A. J. Alazemi, M. I. Waly, R. Ghayoula and S. Kim, "Wideband Wearable Antenna for Biomedical Telemetry Applications," in IEEE Access, vol. 8, pp. 15687-15694, 2020.
- [5] G. -P. Gao, C. Yang, B. Hu, R. -F. Zhang and S. -F. Wang, "A Wide-Bandwidth Wearable All-Textile PIFA With Dual Resonance Modes for 5 GHz WLAN Applications," in IEEE Transactions on Antennas and Propagation, vol. 67, no. 6, pp. 4206-4211, June 2019.
- [6] M. -C. Tang, T. Shi and R. W. Ziolkowski, "Flexible Efficient Quasi-Yagi Printed Uniplanar Antenna," in IEEE Transactions on Antennas and Propagation, vol. 63, no. 12, pp. 5343-5350, Dec. 2015.
- [7] S. Das and D. Mitra, "A Compact Wideband Flexible Implantable Slot Antenna Design With Enhanced Gain," in IEEE Transactions on Antennas and Propagation, vol. 66, no. 8, pp. 4309-4314, Aug. 2018.
- [8] A. Arif, M. Zubair, M. Ali, M. U. Khan and M. Q. Mehmood, "A Compact, Low-Profile Fractal Antenna for Wearable On-Body WBAN Applications," in IEEE Antennas and Wireless Propagation Letters, vol. 18, no. 5, pp. 981-985, May 2019.
- [9] A. S. M. Alqadami, A. E. Stacombe, K. S. Bialkowski and A. Abbosh, "Flexible Meander-Line Antenna Array for Wearable Electromagnetic Head Imaging," in IEEE Transactions on Antennas and Propagation, vol. 69, no. 7, pp. 4206-4211, July 2021.
- [10] Abdullah G. Al-Sehem, Ahmed A. Al-Ghamdi, Nikolay T. Dishovsky, Nikolay T. Atanasov & Gabriela L. Atanasova (2017) Flexible and small wearable antenna for wireless body area network applications, Journal of Electromagnetic Waves and Applications, 31:11-12, 1063-1082.
- [11] Y. J. Li, Z. Y. Lu and L. S. Yang, "CPW-Fed Slot Antenna for Medical Wearable Applications," in IEEE Access, vol. 7, pp. 42107-42112, 2019.
- [12] C. K. Nanda, S. Ballav, A. Chatterjee and S. K. Parui, "A Body Wearable Antenna Based on Jeans Substrate with Wide-Band Response," 2018 5th International Conference on Signal Processing and Integrated Networks (SPIN), Noida, India, 2018, pp. 474-477.
- [13] W. El Hajj, C. Person and J. Wiart, "A Novel Investigation of a Broadband Integrated Inverted-F Antenna Design; Application for Wearable Antenna," in IEEE Transactions on Antennas and Propagation, vol. 62, no. 7, pp. 3843-3846, July 2014.
- [14] I. Gil & R. Fernández-García (2017) Wearable PIFA antenna implemented on jean substrate for wireless body area network, Journal of Electromagnetic Waves and Applications, 31:11-12, 1194-1204.
- [15] "IEEE Standard for Safety Levels with Respect to Human Exposure to Electric, Magnetic, and Electromagnetic Fields, 0 Hz to 300 GHz," in IEEE Std C95.1-2019 (Revision of IEEE Std C95.1-2005/ Incorporates IEEE Std C95.1-2019/Cor 1-2019) , vol., no., pp.1-312, 4 Oct. 2019.
- [16] Noor, Shehab & Ramli, Nurulazlina & Hanapi, Nurul. (2020). A Review of the Wearable Textile-Based Antenna using Different Textile Materials for Wireless Applications. Open Journal of Science and Technology. 3. 10.31580/ojst.v3i3.1665.
- [17] C. A. Balanis, Antenna theory: analysis and design. John wiley & sons, 2015
- [18] A. Y. I. Ashyap et al., "Robust and Efficient Integrated Antenna With EBG-DGS Enabled Wide Bandwidth for Wearable Medical Device Applications," in IEEE Access, vol. 8, pp. 56346-56358, 2020.
- [19] M. Wang et al., "Investigation of SAR Reduction Using Flexible Antenna With Metamaterial Structure in Wireless Body Area Network," in IEEE Transactions on Antennas and Propagation, vol. 66, no. 6, pp. 3076-3086, June 2018.
- [20] H. Yang and X. Liu, "Wearable Dual-Band and Dual-Polarized Textile Antenna for On- and Off-Body Communications," in IEEE Antennas and Wireless Propagation Letters, vol. 19, no. 12, pp. 2324-2328, Dec. 2020.
- [21] X. Lin, Y. Chen, Z. Gong, B. -C. Seet, L. Huang and Y. Lu, "Ultrawideband Textile Antenna for Wearable Microwave Medical Imaging Applications," in IEEE Transactions on Antennas and Propagation, vol. 68, no. 6, pp. 4238-4249, June 2020.
- [22] R. B. V. B. Simorangkir, Y. Yang, K. P. Esselle and B. A. Zeb, "A Method to Realize Robust Flexible Electronically Tunable Antennas Using Polymer-Embedded Conductive Fabric," in IEEE Transac-

-
- tions on Antennas and Propagation, vol. 66, no. 1, pp. 50-58, Jan. 2018.
- [23] R. Joshi et al., "Dual-Band, Dual-Sense Textile Antenna With AMC Backing for Localization Using GPS and WBAN/WLAN," in IEEE Access, vol. 8, pp. 89468-89478, 2020.
- [24] H. Li, S. Sun, B. Wang and F. Wu, "Design of Compact Single-Layer Textile MIMO Antenna for Wearable Applications," in IEEE Transactions on Antennas and Propagation, vol. 66, no. 6, pp. 3136-3141, June 2018.
- [25] A. Iqbal, A. Smida, A. J. Alazemi, M. I. Waly, N. Khaddaj Mallat and S. Kim, "Wideband Circularly Polarized MIMO Antenna for High Data Wearable Biotelemetric Devices," in IEEE Access, vol. 8, pp. 17935-17944, 2020.
- [26] Mustafa, A.B., Rajendran, T. An Effective Design of Wearable Antenna with Double Flexible Substrates and Defected Ground Structure for Healthcare Monitoring System. *J Med Syst* 43, 186 (2019).